PHYSICAL REVIEW B VOLUME 24, NUMBER 8 15 OCTOBER 1981

Applicability and limitations of the phonon-focusing theory based on geometrical acoustics

Shin-ichiro Tamura and Yoshito Nakane
Department of Engineering Science, Hokkaido University, Sapporo 060, Japan
(Received 24 April 1981)

A detailed discussion is given on the applicability and limitations of the naive phonon-focusing theory by Taylor, Maris, and Elbaum. Comparing it with the characteristic behavior of ballistic-phonon propagations detected recently in heat-pulse experiments, we find that the theory predicts correctly the locations of various sharp peaks observed in flux enhancement of transverse phonons. When emissivity of phonons excited in a heat source into an anisotropic crystal is properly taken into consideration, the relevant theory accounts quantitatively for (a) the relative magnitudes of highly enhanced phonon flux of different polarizations measured along the principal crystallographic axes (i.e., the [001], [110], and [111] axes) of a cubic crystal, and (b) the angular dependence of the phonon intensity for the longitudinal mode. On the contrary, in the neighborhood of sharp peaks of the flux, the theory becomes invalid by yielding much larger intensity than that observed in the experiments, which suggests the breakdown of geometrical acoustics on surfaces called caustics.

I. INTRODUCTION

Elastic properties of crystalline solids are anisotropic in general. Propagation characteristics of acoustic phonons in crystals are substantially influenced by the elastic anisotropy. A remarkable feature for ballistic-phonon propagations in anisotropic solids in contrast to those of isotropic ones may be the fact that the energy flow of the phonons given by the group velocity is not necessarily collinear with the phase velocity parallel to the wave vector. Consequently, even if the phonons excited in a crystal are assumed to be distributed uniformly in the wave-vector space, their energy flux will be preferentially concentrated along certain crystallographic directions and deconcentrated along others. This phenomenon was demonstrated many years ago by Taylor *et al.* in experiments employing heat pulses and termed "phonon focusing."[1,2]

Recent experimental investigations of Kapitza thermal resistance[3] and of motions of electron-hole droplets via phonon-wind mechanism[4] seem to renew interest in the focusing of high-frequency incoherent phonons in various dielectric solids. Especially, Hensel and Dynes have studied through their high-resolution heat-pulse experiment the angular dependence of ballistic-phonon amplitudes in Ge.[5] They have found that transverse phonons are focused into sharply defined beams along the [001] and [110] axes and, in particular, these beams display fine structures representing focusing singularities. The same kind of observations has also been made by Northrop and Wolfe with a heat-pulse imagining technique.[6,7]

We believe that an interpretation of these rather complex behaviors of the phonon beams in the ballistic regime should be made by means of the basic theory of the phonon focusing. Actually, the experimental results have partly been explained by following the original ideas of Taylor *et al.*[5,7] Here, we note that this traditional phonon-focusing theory is constructed on the focusing factor introduced by Maris[8] as a ratio of solid angles occupied by the phonons in the wave-vector and real spaces. The focusing factor measures an enhancement of the phonon flux in a specified direction relative to the magnitude it would have in an isotropic medium. However, it is evident that the focusing factor defined in this way is based on a trajectory picture for the phonons or geometrical acoustics,[9] and its analytical expression has been recognized to yield infinities (though integrable) along certain crystal axes. Taborek and Goodstein have remarked that vectors parallel to such crystallographic directions form conical surfaces called caustic surfaces or simply caustics in classical wave theories.[10,11] According to their analysis, the correct phonon intensity obtained by solving the wave equation of the lattice is finite along these directions, though still

enhanced heavily.[10–12] This means that geometrical acoustic approximation breaks down on the caustics.

Recently, considerable efforts have been made to understand the origins of sharp enhancements of the observed phonon flux in connection with the infinities of the focusing factor and the underlying geometry of constant-frequency surfaces of the phonons in the wave-vector space.[7,11] However, no quantitative analysis of phonon intensity beyond the rather early work by Taylor *et al.*[2] has been developed up to the present. They found that the calculated intensities along high-symmetry axes of various crystals are qualitatively in agreement with measured ones. But it is still indefinite whether their naive theory may predict quantitatively correct intensities along any crystallographic directions including the caustics, when the finite aperture effects of the detector are properly taken into account.

The purpose of the present work is then to discuss in detail the applicability of the above-mentioned phonon-focusing theory to analyzing the observed spectrum of long-wavelength phonons in crystals. Here, we note that besides the phonon-focusing effects resulting from crystallographic properties of a solid, the precise understanding of the phonon intensity of the heat-pulse experiments in ballistic regime requires knowledge of (i) distributions of the phonons inside the heater, (ii) transmissions and subsequent refractions of the phonons through heater-crystal and crystal-detector interfaces, and (iii) temporal and spatial resolutions of the detector as well as other possible very minor effects. As we shall see in the following, these effects play very important roles in our investigations. More specifically, the correct estimation for phonon density in the heater is indispensable, in particular, for discussing relative magnitudes of the phonon flux of different polarizations, and the angular dependence of the phonon intensity is governed by the anisotropy of the transmission rate of the phonons across those boundaries.

The organization of this paper is as follows. In Sec. II we give three-dimensional representations of the focusing factor evaluated for three phonon modes in Ge. In particular, the focusing factors versus crystallographic directions in the $(1\bar{1}0)$ plane are illustrated in more detail and they reveal a certain number of sharp peaks in the transverse modes, whose locations are closely coincident with those observed equally in the experiment.[5] The geometrical interpretation of the focusing factor is made, and then origins of these peaks are traced on the constant-frequency surfaces in the wave-vector space of the transverse phonons. Subsequently, the identification of flat points which correspond to the singular enhancements of the phonon flux in the $(1\bar{1}0)$ plane is tried, taking solid-angle effects subtended by the detector carefully into account. The effects of phonon transmissions at a heater-crystal interface upon the focusing will be considered in Sec. III. This amounts to correcting the angular distribution of phonon wave vectors in the crystal which is implicitly assumed to be uniform in the evaluation of the focusing factor in Sec. II. We also incorporate in the calculation the relative abundance of the phonons of three possible polarizations excited in the phonon source. Relative magnitudes of phonon intensity between the longitudinal and transverse phonons, and the angular dependence of the intensity for the longitudinal mode in the $(1\bar{1}0)$ plane are then studied with the aid of extensive numerical calulations. Finally, in Sec. IV we summarize the results and give conclusions.

II. ENHANCEMENT AND SINGULAR BEHAVIOR OF PHONON FLUX

In this section we shall discuss how the substantial aspects of the experiments[5–7] such as sharp peaks, broad bumps, and other features found in the data of phonon amplitudes versus crystallographic directions can be accounted for by applying the basic idea of the phonon focusing due to crystal anisotropy. The analysis is largely based on the focusing factor of the phonon flux defined by $A=\Delta\Omega_{\vec{k}}/\Delta\Omega_{\vec{w}}$ in the limit $\Delta\Omega_{\vec{k}},\Delta\Omega_{\vec{w}}\rightarrow 0$, where $\Omega_{\vec{k}}$ denotes a solid angle in wave-vector space ($\vec{k}$ indicates a wave vector) occupied by the phonons and $\Omega_{\vec{w}}$, a solid angle subtended by the corresponding group velocity $\vec{w}$ in real space. An analytic expression for A in terms of amplitudes and phase velocities of acoustic fields was derived by Maris.[8] Unfortunately, it is hard to apply the formula directly to transverse phonons because the phonon flux of a transverse mode in a given direction consists generally of more than one phonon traveling with group velocities different in magnitudes. Hence, in the calculation of the focusing factor we employed the coarse-grained statistical method devised by Taylor *et al.*[2] The explicit procedure is just the same as that of Ref. 5. In short, we subdivided the polar (θ) and azimuthal (ϕ) coor-

dinates both in the wave-vector and real spaces to make finite but fine angular meshes $(\Delta\theta,\Delta\phi)$ of (0.05°,0.05°) and (0.5°,0.5°), respectively. Next, assigning a factor $\sin\theta_{\vec{k}}$ to each mesh in the former space, we counted the number of meshes (weighted with $\sin\theta_{\vec{k}}$ in the wave-vector space which are mapped onto each mesh in the real space. The result when divided by $\sin\theta_{\vec{w}}$ yields the focusing factor along a $\vec{w}$ direction. In the course of the calculation we have used a closed-form expression for the phase and group velocities given by Every, which saves computation time considerably.[13]

Three-dimensional representations of the focusing factor for three phonon polarizations in Ge are shown in Figs. 1(a)—1(c), where the angular resolutions of $\pm 0.25°$ in the polar direction and of $\pm 1°$ in the azimuthal direction are assumed.[14] It should be noted that, in our calculation, two quasi-transverse modes of the phonons are classified by the speeds of their phase velocities but not of group velocities, that is, $T1$ denotes a transverse phonon with a slower phase velocity and $T2$ with a faster one (a longitudinal phonon is denoted by LA). We immediately recognize various narrow focusing peaks in both transverse phonons but rather broad humps in longitudinal phonons. In order to interpret the calculated results in comparison with measured phonon intensity, we have illustrated in Fig. 2 the focusing factor in the $(1\bar{1}0)$ plane integrated over $\pm 3°$ (not over $\pm 1°$) normal to this plane. The assumed angular resolution is accommodated to the experimental situation.[5]

Apart from the overall magnitudes, the results of Fig. 2 qualitatively describe the phonon amplitudes observed by Hensel and Dynes.[5] More precisely, as in the experimental results, we find two abrupt amplifications of phonon flux at 7.5° and 2° measured from the [001] and [110] directions, respectively, and other three peaks at 5.5° rotated away from the [001] direction and at $\pm 6°$ ($\pm 5.5°$ in the experiment[5]) on either side of the [111] direction. The positions of the first three peaks are identical to the experimental data up to assumed uncertainties of the statistical calculation. Thus, with respect to the peak locations of the phonon flux the coincidence of the theory with the experiment is remarkable. Here, we mention that the noticeable behaviors of the phonon focusing of $T1$ mode near the [001] direction have already been established by the same kind of calculations,[5,7] but the remaining structures for three phonon modes have not yet been analyzed in detail.

For pedagogical purposes we shall discuss how

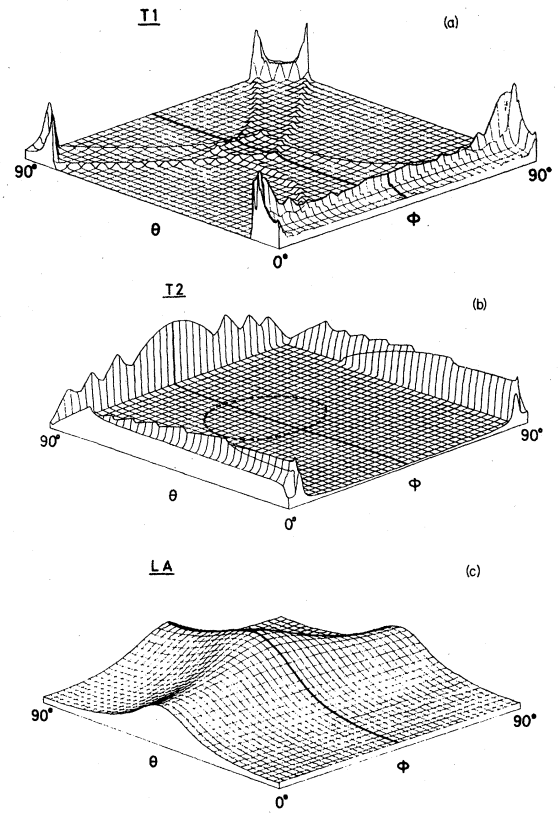

FIG. 1. Three-dimensional representations of the focusing factor of Ge integrated over $\pm 0.25°$ in the θ direction and $\pm 1°$ in the ϕ direction. (Angles θ and ϕ refer to the polar and azimuthal angles measured from the [001] and [100] directions, respectively). (a) $T1$ (transverse mode with slower phase velocity) phonon, (b) $T2$ (transverse mode with faster phase velocity) phonon, and (c) LA (longitudinal-mode) phonon. Note that ridges in (a) around the [111] direction ($\theta=\tan^{-1}\sqrt{2}$ $\simeq 54.7°$, $\phi=45°$) terminate making cuspidal edges at (θ,ϕ) $=(47°,45°)$, (60°,53°), and (60°,37°). Inside the broken circle of (b) the focusing factor vanishes (i.e., completely defocusing region). Bold solid lines are the traces of the focusing factor in the $(1\bar{1}0)$ plane.

the origins and their locations of the peaks found in the transverse phonons are explained by referring to the underlying topological properties of the focusing factor. To begin with we show that the focusing factor A defined by the ratio of the solid angles depends on the curvature of a constant-frequency surface (ω surface) in the wave-vector space. When the ω surface of a phonon with certain polarization is expressed in the form

$$k_3=f(\vec{k}_{||})\,, \tag{1}$$

with $\vec{k}_{||}=(k_1,k_2)$ where the wave vector

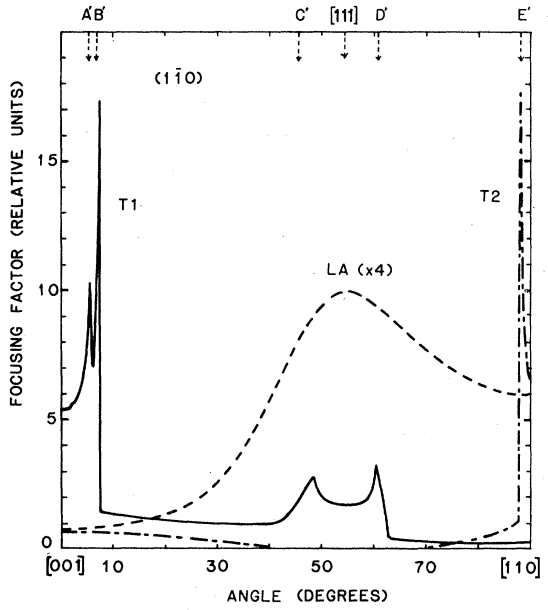

FIG. 2. Angular dependence of the focusing factor in the (1$\bar{1}$0) plane of Ge integrated over $\pm 0.25°$ and $\pm 3°$ within and perpendicular to the (1$\bar{1}$0) plane, respectively. Note that the longitudinal mode is multiplied by four. Analytical expression of the focusing factor becomes singular at directions marked $A'-E'$.

$\vec{k}=(\vec{k}_{||},k_3)$ is defined with reference to a local Cartesian coordinate system fixed on the surface, it can be readily deduced that

$$A^{-1}=\frac{\cos\Theta_{\vec{k}}}{\cos\Theta_{\vec{w}}}\,|\vec{k}|^2K\ , \tag{2}$$

where

$$K=\frac{f_{11}f_{22}-f_{12}^2}{(1+f_1^2+f_2^2)^2}\ , \tag{3}$$

with $f_i\equiv\partial f/\partial k_i$, and $f_{ij}\equiv\partial^2 f/\partial k_i\partial k_j$ is the Gaussian curvature of the ω surface and $\Theta_{\vec{k}}$ ($\Theta_{\vec{w}}$) is the polar angle of the wave vector (the group velocity) measured from the third axis in the wave-vector space. Since the Gaussian curvature is a geometric invariant of the surface it is convenient to choose the k_3 axis being normal to the ω surface. In this case $\Theta_{\vec{w}}$ is identical to zero because the group velocity by its definition is directed perpendicular to the ω surface, or parallel to the k_3 axis, and we have

$$A^{-1}=|\vec{k}|^2K\cos\Theta\ , \tag{4}$$

where Θ refers to the angle between the group velocity and the wave vector.

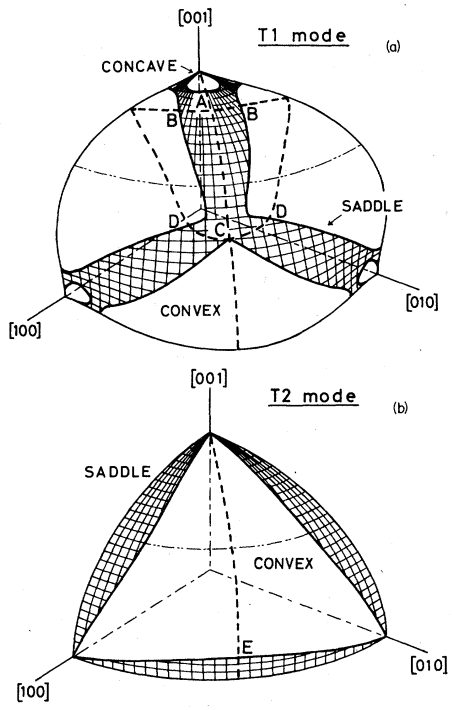

FIG. 3. Constant-frequency surfaces (ω surfaces) of (a) $T1$ phonon and (b) $T2$ phonon of Ge. Bold solid curves separate the regions of negative curvature (saddle) from those of positive curvature (convex and concave) on the ω surfaces. Broken curves are traces of points on the ω surfaces at which normal vectors are parallel to the (1$\bar{1}$0) plane. Intersections $A-E$ of these curves give rise to singularities of the focusing factor in the (1$\bar{1}$0) plane. The directions of normals at $A-E$ are indicated by $A'-E'$, respectively, in Fig. 2.

Based on the above consideration the focusing factor of the phonon flux is seen to be singular along directions normal to the ω surface at points of zero curvature ($K=0$). The group velocities at such flat points on the ω surface sweep out conical surfaces called caustic surfaces or simply caustics.[10] On the caustics the focusing factor A derived in the framework of the geometrical acoustics blows up. In our evaluation, however, the phonon flux has been integrated over a finite solid angle $\Delta\Omega_{\vec{w}}$. Accordingly, it would be expected that large but finite peaks rather than singularities are obtained along directions on the caustics. The five peaks that appeared in the focusing of the transverse phonons in the (1$\bar{1}$0) plane are then likely to be large amplifications of the phonon flux predicted in caustic directions. In order to convince ourselves that this is indeed the case, we have depicted in Figs. 3(a) and 3(b) three-dimensional representations of the ω surfaces for both transverse modes of Ge, which

are drawn according to a perspective projection viewed from a polar angle $\theta=60°$ and an azimuthal angle $\phi=29°$.

Bold solid curves in these figures are traces of the flat points on the ω surfaces and separate saddle regions with negative curvature ($K<0$) from convex or concave regions with positive curvature ($K>0$). On the other hand, broken curves show positions of points on the ω surfaces at which the group-velocity vectors become parallel to the $(1\bar{1}0)$ plane. Therefore, the outward normals at the points on the ω surfaces where both the solid and broken curves intersect give the caustic directions in the $(1\bar{1}0)$ plane. As can be seen from Figs. 3(a) and 3(b), there are four (marked with A to D) and only one (marked with E) points of zero curvature on the ω surfaces of the $T1$ and $T2$ modes, respectively, which should contribute to the strong focusing of the phonons in the $(1\bar{1}0)$ plane of Ge. The directions in the real space of the group velocities at the points A to E are indicated by A' to E' in Fig. 2 and their angles in the $(1\bar{1}0)$ plane measured from the [001] axis are given in Table I. The coincidence of these directions with locations of the peaks of the focusing factor are prominent except for C' and D'. The latter modest deviations, however, are due to finite solid-angle effects of the detector. This can be best understood by reevaluating the focusing factor assuming a finer angular resolution of the detector. Results tell us that the peaks gained by the calculation at about $\pm6°$ on either side of the [111] direction of the $T1$ mode are modified considerably both in their magnitudes and locations, whereas no appreciable change takes place elsewhere. In Fig. 4 the focusing factor of the $T1$ phonons versus the polar angle near the [111] direction is plotted for two different values, namely, $\pm1°$ and $\pm3°$ of the angular resolution normal to the $(1\bar{1}0)$ plane. We find that the position of each peak is much closer to C' or D' when the resolution is in a higher level. Another interesting observation is that the relative peak height is interchanged between these two curves. It should be noted that the relative magnitude of peak heights in the solid curve obtained for the resolution of $\pm3°$

TABLE I. Directions measured from the [001] axis along which the focusing factor becomes singular in the $(1\bar{1}0)$ plane of Ge.

A'	B'	C'	D'	E'
7.4°	5.7°	45.5°	61.3°	88.0°

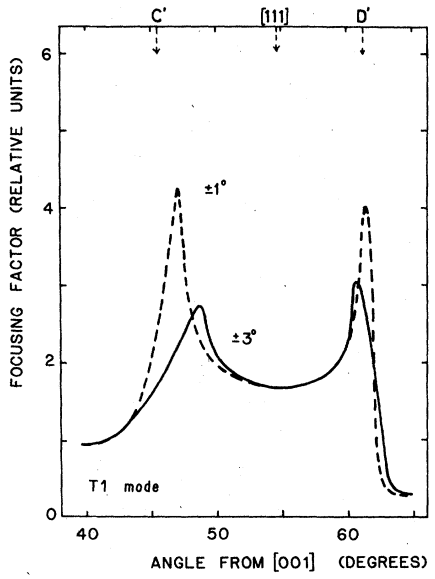

FIG. 4. Focusing factors of $T1$ phonon near the [111] axis integrated over $\pm3°$ (solid curve) and $\pm1°$ (broken curve) perpendicular to the $(1\bar{1}0)$ plane of Ge.

is qualitatively in agreement with the experimental observations.[5]

Following the analysis being made hitherto, it may be confirmed that observed sharp focusings of the phonon flux correspond to the infinities of the focusing factor arising in the approximation of geometrical acoustics and are deeply connected with topological properties of the ω surfaces. The existence of various ridges found in the maps of Figs. 1(a) and 1(b) will be equally explained by referring to the shapes of the complete ω surfaces. A similar conclusion has been reached by Northrop and Wolfe.[7] To sum up, the naive idea of the focusing based on the ray picture of the phonons predicts the appearance of the sharp peaks of the phonon flux and their proper loci measured in the heat-pulse experiments. In addition, the solid-angle effects of the detector play significant roles in predicting quantitatively correct locations of relevant flux peaks.[15]

III. EFFECTS OF PHONON TRANSMISSION AND COMPARISON OF INTENSITY

In the discussion of the phonon-focusing effects developed in the preceding section, the following have been assumed tacitly. Firstly, immediately after the excitation in a crystal the angular distribution of phonons in the wave-vector space is uni-

form, and secondly, the relative abundance of the phonons in the crystal is equal, irrespective of their polarizations. However, none of the above-mentioned simplifications are applicable to quantitative studies of measured phonon intensity in the heat-pulse experiments. This is because the density of the phonons generated in a heater depends largely on their polarizations and a certain amount of the phonons incident on the heater-crystal boundary are reflected back to the heater due to the presence of acoustic mismatch.

Hence, in order to discuss the phonon intensity we must explicitly take into account the density of the phonons excited in the heater and their incomplete (and also anisotropic) transmissions into the crystal. In the work of Taylor *et al.* these effects were only estimated by approximating both the heater and the crystal to be isotropic in their elastic properties.[2]

Now, we note that an incoming phonon beam of a definite polarization falling upon a heater-crystal interface can generate, in general, three transmitted phonon beams of different polarizations. On the other hand, an outgoing phonon beam of a specified polarization may be produced by three incoming phonon beams in the heater. Accordingly, introducing the phonon flux F^H in the heater (H) and F^C emitted into the crystal (C), which are defined per unit solid angle in the wave-vector space, we have[16]

$$F^C(\omega,\vec{k}^C,\lambda)d\Omega(\vec{k}^C,\lambda)=\sum_{\sigma=\{T1,T2,\mathrm{LA}\}} t_{\lambda\sigma}(\vec{k}^C,\vec{k}^H)F^H(\omega,\vec{k}^H,\sigma)d\Omega(\vec{k}^H,\sigma)\ , \tag{5}$$

where ω is the angular frequency of the phonons and

$$d\Omega(\vec{k}^C,\lambda)=-d[\cos\theta(\vec{k}^C,\lambda)]d\phi(\vec{k}^C,\lambda)$$

stands for an infinitesimal solid angle about a wave vector $\vec{k}^C$ of the phonons with polarization λ in the crystal, which is related to the solid angle $d\Omega(\vec{k}^H,\sigma)$ of incident phonons with polarization σ in the heater (the polar angle θ is measured from the normal of the interface). The quantity denoted by $t_{\lambda\sigma}$ is a transmission coefficient of the phonons defined by $t_{\lambda\sigma}=p^C_\lambda/p^H_\sigma$, where p^C_λ (p^H_σ) is the component normal to the interface of the Poynting vector associated with the phonons of the polarization λ (σ) in the crystal (heater). Three possible sets of $\vec{k}^H$ and σ connected with a given $\vec{k}^C$ and λ are determined uniquely by boundary conditions at the interface. It should be remarked that F^C and F^H are not directly observable in contrast to the phonon flux in the real space. For the sake of the following discussions, here we shall give the relationship between the phonon flux F in the wave-vector space and f in the real space

$$F^i(\omega,\vec{k}^i,\lambda)d\Omega(\vec{k}^i,\lambda)=f^i(\omega,\vec{e}^i,\lambda)d\Omega(\vec{e}^i,\lambda)\ , \tag{6}$$

with $i=C$ and H, where $\vec{e}^i\equiv\vec{w}(\vec{k}^i)/|\vec{w}(\vec{k}^i)|$ is the unit vector parallel to the group velocity $\vec{w}(\vec{k}^i)$, and $d\Omega(\vec{e}^i,\lambda)$ is the corresponding infinitesimal solid angle subtended in the real space.

Next, with a commonly used approximation we assume that soon after the thermalization the phonons in the heater are in an equilibrium state characterized by an appropriate temperature T. Then the flux F^H in the heater which impinges on the interface of area S may be expressed as

$$F^H(\omega,\vec{k}^H,\sigma)=\frac{S}{(2\pi)^3}\omega^2 n(\omega,T)\frac{\cos\theta(\vec{k}^H,\sigma)}{(v^H_\sigma)^2}\ , \tag{7}$$

where n is the Planck distribution function and v^H_σ is the phase velocity of the phonons with polarization σ in the heater. In deriving Eq. (7) it is also assumed that the heater (an evaporated Constantan film on the crystal[5]) is elastically isotropic and, therefore, no $\vec{k}^H$ dependence is present in v^H_σ. Equation (7) tells us that the ratio of the longitudinal and degenerate transverse ($T1=T2\equiv\mathrm{TA}$) phonons incident along the same direction on the heater-crystal interface is given by $(v^H_{\mathrm{TA}}/v^H_{\mathrm{LA}})^2$ and it leads to suppression of the observed flux for the longitudinal mode.

For further calculations we note that

$$\frac{d\Omega(\vec{k}^H,\sigma)}{d\Omega(\vec{k}^C,\lambda)}=\frac{v^H_\sigma}{v^C_\lambda(\vec{k}^C)}\frac{d\theta(\vec{k}^H,\sigma)}{d\theta(\vec{k}^C,\lambda)}=\left[\frac{v^H_\sigma}{v^C_\lambda(\vec{k}^C)}\right]^3\frac{1}{v^H_\sigma\cos\theta(\vec{k}^H,\sigma)}\frac{dv_{\|}}{d\kappa}\ , \tag{8}$$

where v_λ^C is a phase velocity of the phonons in the crystal,

$$v_{||} \equiv v_\sigma^H / \sin\theta(\vec{k}^H,\sigma) = v_\lambda^C(\vec{k}^C)/\sin\theta(\vec{k}^C,\lambda)$$

is a phase velocity projected on the interface, and κ defined by $\kappa \equiv \cot\theta(\vec{k}^C,\lambda)$ is related to a component perpendicular to the interface of the direction cosine of $\vec{k}^C$. Accordingly, expression (5) together with Eqs. (7) and (8) leads to

$$F^C(\omega,\vec{k}^C,\lambda) = \frac{B(\omega,T)}{(v_\lambda^C)^3}\frac{dv_{||}}{d\kappa}\sum_\sigma t_{\lambda\sigma}(\vec{k}^C,\vec{k}^H) , \tag{9}$$

where $B(\omega,T)=S\omega^2 n/(2\pi)^3$ is a factor depending on the temperature and the frequency of the phonons in the heater, and its explicit expression is irrelevant in the following discussions. Equation (9) gives the magnitude and the angular dependence of the phonon flux in the wave-vector space of the crystal. The derivative $dv_{||}/d\kappa$ entering in this equation should be identified physically with the component of the group velocity normal to the interface. We shall show in the Appendix that this is indeed the case.

Now, with the aid of Eq. (6) the phonon intensity I^C per unit solid angle along a direction $\vec{e}^C$ in the crystal may be written in terms of the phonon flux F^C given by Eq. (9), and the focusing factor A computed previously as

$$\begin{aligned} I^C(\omega,\vec{e}^C,\lambda) &= \sum \hbar\omega f^C(\omega,\vec{k}^C,\lambda) \\ &= \sum \hbar\omega F^C(\omega,\vec{k}^C,\lambda) A[\vec{w}(\vec{k}^C)] , \end{aligned} \tag{10}$$

where the summation should be taken over the wave vector $\vec{k}^C$ in the crystal for which the group velocity $\vec{w}$ is collinear with the unit vector $\vec{e}^C$.

Finally, we are left to obtain the transmission coefficients t's in Eq. (9). In principle, they can be evaluated in the framework of continuum elastic theory by solving the equations of motion for lattice displacements both in the heater and the crystal as well as the boundary conditions at the interface. It may be worthwhile to note that the acoustic mismatch model is appropriate to describe transmissions of the phonons through a solid-solid interface at low heater power or low-frequency excitation.[17] For explicit calculations of those transmission coefficients, we should initially understand the experimental arrangements of the heater and the detector relative to the crystal. As is shown in Fig. 5, the heater-crystal boundary of the

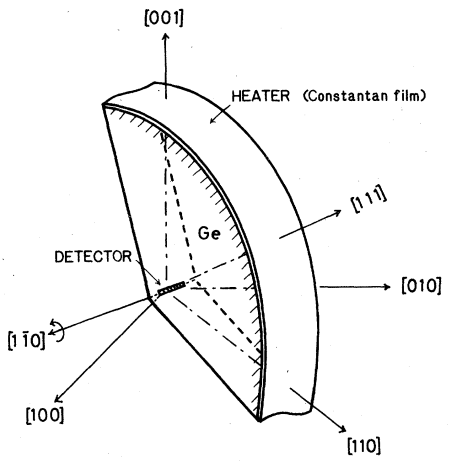

FIG. 5. Schematic drawing of the geometrical arrangement for the detection of ballistic-phonon focusing by Hensel and Dynes. (Ref. 5). Heat pulses are generated optically by a laser beam focused on the cylindrical surface which is coated with an evaporated Constantan film. The detector placed parallel to the [1$\bar{1}$0] axis is an Al superconducting bolometer with the dimensions 0.1×1.0 mm^2. The radius of the sample (Ge) is 1 cm.

experiment[5] is not flat but in the shape of cylindrical surface so that the normal of the interface may rotate smoothly from the [001] to [110] directions via the [111] one in the (1$\bar{1}$0) plane of Ge. Furthermore, we note that the detector (a thin-film granular Al superconducting bolometer[5]) is in the form of a narrow strip and is put at the center of the cylinder (Ge sample) aligned with the [1$\bar{1}$0] axis (the axis of rotation).

If we take these circumstances into account, it seems to be a difficult task to determine in a straightforward fashion the sum in Eq. (9) of appropriate transmission coefficients from the heater to the crystal, because it is not $\vec{k}^H$ but $\vec{k}^C$ which is directly connected with the phonons to be observed. Fortunately, however, the reciprocity relation $t_{\lambda\sigma}(\vec{k}^C,\vec{k}^H) = t_{\sigma\lambda}(\vec{k}^H,\vec{k}^C)$ holds for the transmission coefficient. This means that when the modes λ and σ and the wave vectors $\vec{k}^C$ and $\vec{k}^H$ of the phonons being linked together at the boundary are specified, the transmission rate from the heater to the crystal is identical to that from the crystal to the heater. The application of this equation considerably facilitates practical calculations of the flux F^C's excited in the crystal, that is, when we find a pertinent $\vec{k}^C$ among a number of wave vectors on an ω surface we may just evaluate the transmission coefficients of the corresponding phonon into three kinds of phonons in the heater, in-

stead of computing those from the heater to the crystal.

In the above scheme, sums of the transmission coefficients and in turn the flux F^C's are calculated by considering carefully the arrangements of the heater and the detector. Plotted in Fig. 6 are relative magnitudes of F^C's in the $(1\bar{1}0)$ plane (in the real space) of Ge which are radiated from the Constantan film.[18] For transverse modes the phonon flux reveals a folded structure and consists of multiple branches. A branch of the $T1$ mode drawn with the solid curve shows the flux accompanied by the phonons with their wave vectors within the $(1\bar{1}0)$ plane, and that with the dot-dash curve originated from the phonons with their wave vectors out of this plane. In this figure we also marked with A' to E' the flux in the directions along which the $(1\bar{1}0)$ plane and the caustics of the transverse phonons in Ge intersect. It is interesting to note that these curves are folded at A', B', D', and E', whereas two branches coalesce at C'. As can be seen in Fig. 1(a), a pair of ridges of the focusing factor terminate and make a cuspidal structure in the direction corresponding to C', but they only traverse the $(1\bar{1}0)$ plane in the other directions.

For the longitudinal mode the phonon flux is single valued in every crystallographic direction of Ge, and the emissivity defined by the ratio of F^C's is given by 1:0.81:0.85 along the [001], [111], and [110] directions, respectively. The flux of the longitudinal phonons emitted from the heater as compared to those of the transverse phonons is largely suppressed mainly due to the factor $(v_\lambda^C)^{-3}(dv_{||}/d\kappa) \simeq (v_\lambda^C)^{-3} \mid \vec{w} \mid$ of Eq. (9) and will lead to overall reduction of the LA-phonon intensity in the heat-pulse experiments.

The phonon intensity in the crystal is obtained by combining the focusing factor with the emissivity of the phonons across the heater-crystal boundary according to Eq. (10). The result in the $(1\bar{1}0)$ plane is shown in Fig. 7. Compared with the focusing factors in Fig. 2, the effects of the phonon transmission on the relative intensities among the longitudinal and transverse phonons are now evident and hardly require comment.

For quantitative comparison of the theory with the experiment[5] we tablulated in Table II the calculated phonon intensities along principal crystallographic directions together with the experimental results. It can be seen that the theory is in good agreement with the experiment provided a relevant direction coincides with a focusing ($A > 1$) direction of the flux. On the contrary, the agreement is rather poor along defocusing ($A < 1$) directions. The latter disagreement may be expected because

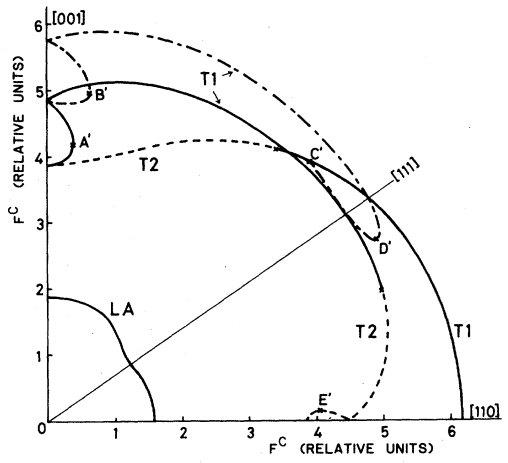

FIG. 6. Flux or emissivity of phonons in the first quadrant of the $(1\bar{1}0)$ plane of Ge which emanates from the adjacent Constantan heater in the configuration of Fig. 5. The solid (dot-dash) curve represents the flux of $T1$ phonons with their wave vectors within (out of) the $(1\bar{1}0)$ plane. For transverse phonons transitions from $T1$ to $T2$ and vice versa happen. The flux of the phonons at points $A-E$ on the ω surfaces in Figs. 3(a) and 3(b) are marked again with $A'-E'$.

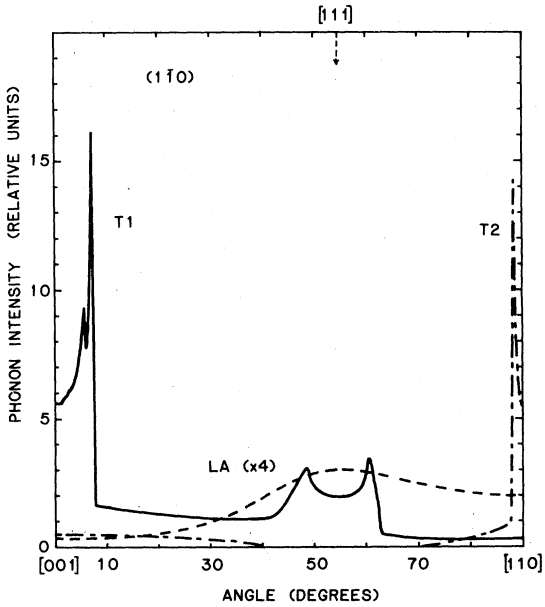

FIG. 7. Calculated phonon intensity in the $(1\bar{1}0)$ plane of Ge. The intensity of the longitudinal phonon (broken curve) is multiplied by 4 and is suppressed considerably in comparison with those of the $T1$ phonon (solid curve) and $T2$ phonon (dot-dash curve).

TABLE II. Relative phonon intensities along principal crystallographic directions of Ge. Calculated values are given in the first row and experimental data (Ref. 5) in the second row in parentheses. Note that in the [001] direction two transverse modes are degenerate and the numerical value (i.e., unity) represents the sum of these modes.

	[001]	[111]	[110]
$T1$		0.31	0.04
		(0.30)	(0.20)
	1		
	(1)		
$T2$		0	0.89
		(0)	(0.90)
LA	0.013	0.12	0.079
	(0.021)	(0.13)	(0.080)

the effects being overlooked hitherto, such as background phonon signals, become much more efficient in the low-intensity, defocusing regions.

The effects on the phonon focusing in the crystal of the anisotropic phonon transmission through the heater-crystal boundary can be best illustrated by studying the angular dependence of the phonon intensity of the longitudinal mode. In Fig. 8 we show normalized intensity versus crystallographic directions of the longitudinal phonons in the $(1\bar{1}0)$ plane of Ge. Dots indicate the data measured by Hensel and Dynes,[5] and the broken curve shows the intensity obtained by assuming the isotropic distribution for the phonon wave vectors in the crystal, or by making the flux F^C in Eq. (10) a constant independent of $\vec{k}^C$. On the other hand, the solid curve represents the theoretical values corrected by the anisotropic phonon transmission from Constantan to Ge and fits the data more closely than the broken curve. Note that both curves are adjusted to the data in the [110] direction. If we take into account the fact that the anisotropy of the phonon transmission across the crystal-detector interface has not been considered in the calculations, it may be concluded that the theory successfully describes the experiments for the longitudinal phonons though the fitting near the [001], or the defocusing direction is again slightly inadequate in the quantitative sense.

The analysis being developed so far seems to support, for the most part, the applicability of the employed theory to the quantitative studies of the

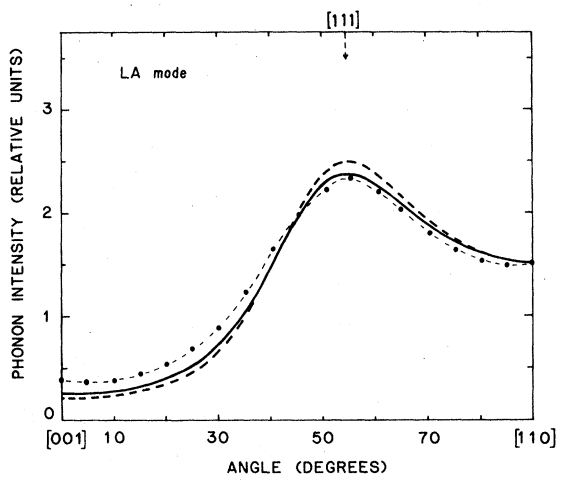

FIG. 8. Angular dependence in the $(1\bar{1}0)$ plane of the phonon intensity of longitudinal mode. The broken curve is the plot of the intensity obtained for isotropic distribution of the wave vectors in the crystal. The solid curve is the plot of the intensity corrected by the anisotropic phonon transmission across the heater (Constantan)-Ge interface. The dots are the experimental data of Ref. 5. These intensities are adjusted to the same value (i.e., 1.5) in the [110] direction.

ballistic phonons in the crystal. However, a crucial feature which limits the predictability of the theory can be seen from Fig. 9 on the relative magnitudes of the ballistic-phonon intensity over the finite range of the propagation directions near the [111] axis. Dots in Fig. 9 represent the measured intensities of the transverse phonons normalized by the calculated LA-phonon intensity. We note that in

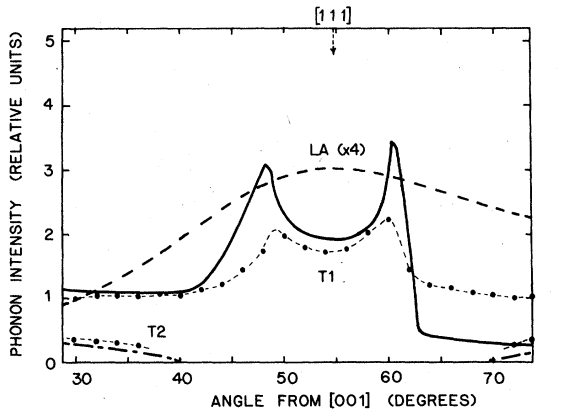

Fig. 9. Magnification of Fig. 7 in the neighborhood of the [111] axis. The dots are the experimental data of transverse phonons (Ref. 5) normalized by the calculated intensity of longitudinal phonon.

the angular range from 40° to 70° rotated away from the [001] direction, the latter intensity describes the experimental results quantitatively (see Fig. 8). Comparing those data with the solid curve which plots the calculated $T1$-phonon intensity, we find large discrepancies between the theory and the experiment in the neighborhood of the directions where the $T1$ mode makes peaks. These disagreements are attributed to an inherent limitation of the approximation for the focusing factor based on the geometrical acoustics, as noted in the foregoing sections, and are therefore present even when the finite solid-angle effects of the detector are properly taken into consideration.

It will be interesting to investigate whether the theory may provide quantitatively reliable intensity for the transverse phonons apart from the caustic directions. The validity of the theory at high-intensity, focusing directions for these phonons has already been confirmed (see Table II). Actually, we recognize in Fig. 9 that for the $T1$ mode the dots and the solid curve are well matched in the vicinity of the [111] axis (the focusing direction) and at angles smaller than 40°. On the contrary, the disagreement of the theory with the experiment is rather remarkable in the defocusing directions of the phonons, namely, at angles larger than 63° for the $T1$ mode. In the context of the assumed focusing model, the focusing factor which measures the enhancement of the phonon flux with respect to that of an isotropic medium should yield 4π when integrated over the whole solid angles in the real space. Then it would be easily envisaged that due to unphysical infinities (though integrable) on the caustics of the employed focusing factor, the theory may predict the phonon flux enhanced excessively in their neighborhoods but suppressed too much elsewhere compared to the flux to be observed. It might be rather surprising that such a theoretical overestimation of the flux near the caustics does not seem to influence the matching of the phonon intensity along the symmetry axes of the crystal provided they coincide with the focusing directions of the phonons.

IV. SUMMARY AND DISCUSSIONS

Through our investigation, first we established that there really exist one-to-one correspondences between the sharp enhancements of the observed phonon flux and the singularities of the focusing factor which are attributed to the flat points on the constant-frequency surfaces of the phonons. In addition, we also ascertained that locations in the real space of those intensity peaks are predicted quantitatively by the theory provided the solid-angle effects of the detector are properly taken into account. It should be noted that the peak positions are crucially dependent upon the spatial resolution of the detector and do not necessarily coincide with the directions normal to the constant-frequency surface at the flat points.

Second, in order to see the validity of the theory for magnitude and angular dependence of the phonon intensity in the crystal, the relative densities in the heater of the phonons with different polarizations as well as their incomplete and anisotropic transmissions into the crystal were combined with the focusing factor. The latter effects are important especially in understanding the angular dependence of the phonon intensity and are studied in detail for the longitudinal mode in which the transmission coefficient is single valued along every possible crystallographic direction. The result supports the theory owing to its close agreement with the experiment. Furthermore, the relative intensities of the phonons calculated in three principal crystallographic axes (the [001], [110], and [111] axes) of Ge uphold again the applicability of the assumed theory. However, in the vicinity of a caustic direction where the intensity makes a peak, the theory gives too large a magnitude of the intensity which is not quantitatively accomodated with the experimental data. Subsequently, it also fails to predict proper intensity, in particular, in the defocusing region apart from the caustics.

On the caustics the analytic expression of the focusing factor yields infinities which are not compatible with the underlying linear theory of elasticity, and a careful analysis, beyond the geometrical acoustics, on the basis of asymptotic phonon fields obtained by solving the wave equation of the lattice is required. According to such an analysis, it has been shown that acoustic fields emanating from a point source decrease more slowly than r^{-1} along the caustic directions, namely, in proportion to $r^{-5/6}$ (corresponding to fold catastrophe) or $r^{-3/4}$ (corresponding to cusp catastrophe) for a large distance r between the source and a point at which the fields are observed.[10] For the longitudinal phonons in Ge, however, no caustic exists and the calculated intensity coincides closely with the experimental results.

The reason why the peak positions of the sharp enhancements of the phonon flux are predicted correctly by finding infinities of the focusing factor

would be now evident. In short, the rigorous treatment of the problem gives rise to the phonon intensity enhanced still heavily along the caustic directions due to much weaker spatial dependence than r^{-1} of the phonon fields.

In the present work, we did not consider emissivity of the phonons from the crystal to the detector (granular Al film in Ref. 5), and the complete acoustic matching at the crystal-detector boundary was assumed. Taking the imperfect phonon transmission through Ge-Al interface into account, we can obtain in practice a much better fitting of the theory to the experiment, for instance, in the angular dependence of the phonon intensity of the longitudinal mode. But we have not displayed the results further. This is partly because we do not have any information about the orientation of the detector normal to a cubic axis and, in addition, about the magnitude of background signals due to diffuse propagations of the phonons, which may be crucial in advancing the quantitative discussions more.

In conclusion, the conventional theory of the phonon focusing based on the geometrical acoustic approximation and the acoustic mismatch model at the phonon source-crystal interface can well account for a number of characteristic behaviors of ballistic phonons observed in the heat-pulse experiments except for their intensities in the neighborhood of the caustics.

ACKNOWLEDGMENTS

The authors would like to thank Prof. T. Sakuma for a critical reading of the manuscript. They also wish to acknowledge the computational help of N. Nishiguchi. This work is supported by a Scientific Research Fund from the Ministry of Education.

APPENDIX

Here, we show that the derivative $dv_{||}/d\kappa$ in Eqs. (8) and (9) is equal to a component normal to the heater-crystal interface of group velocity in a crystal. To start with, let us set a local Cartesian coordinate system such that the x_1-x_2 plane and x_3 axis are tangential and normal to the interface, respectively. Next, we shall write the space and time dependences an acoustic field $\vec{u}$ in the crystal as

$$\vec{u} \propto \exp[i(\vec{k}\cdot\vec{x}-\omega t)] = \exp[ik_{||}(\vec{\kappa}_{||}\cdot\vec{x}_{||}+\kappa_3 x_3 - v_{||}t)] , \tag{A1}$$

where $\vec{x}=(\vec{x}_{||},x_3)$, $\vec{k}=k_{||}(\vec{\kappa}_{||},\kappa_3)$ with $k_{||}=(k_1^2+k_2^2)^{1/2}$ is the wave vector, and ω is the angular frequency of the phonons. We can easily see that $v_{||}$ in this equation is identical to that defined in the text. The two-dimensional vector $\vec{\kappa}_{||}$ is the unit vector which defines the direction cosine of the wave vector mapped onto the interface, and the magnitude of $\vec{k}$ is given by $|\vec{k}|=k_{||}(1+\kappa_3^2)^{1/2}$. Hence $\kappa_3=\cot\theta$ holds (or $\kappa_3=\kappa$ in the text) where θ is the polar angle of $\vec{k}$ measured from the third axis.

Now, from the relation $\kappa_i=k_i/k_{||}$ for $i=1$, 2, and 3, we have

$$\frac{\partial\kappa_j}{\partial k_i}=\frac{1}{k_{||}}(\delta_{ij}-\kappa_i\kappa_j) \quad \text{for } i=1 \text{ and } 2 , \tag{A2}$$

$$\frac{\partial\kappa_j}{\partial k_3}=\frac{1}{k_{||}}\delta_{j3} . \tag{A3}$$

Then, it follows that

$$\frac{\partial\omega}{\partial k_i}=\frac{\partial}{\partial k_i}(v_{||}k_{||})=\begin{cases}\kappa_i v_{||}+k_{||}\dfrac{\partial v_{||}}{\partial k_i} & \text{for } i=1 \text{ and } 2\\ k_{||}\dfrac{\partial v_{||}}{\partial k_3} & \text{for } i=3 .\end{cases} \tag{A4}$$

With the aid of Eqs. (A2) and (A3), Eq. (A4) is reduced to

$$\frac{\partial\omega}{\partial k_i}=\begin{cases}\kappa_i v_{||}+\displaystyle\sum_{j=1}^{3}(\delta_{ij}-\kappa_i\kappa_j)\frac{\partial v_{||}}{\partial\kappa_j} & \text{for } i=1 \text{ and } 2\\ \dfrac{\partial v_{||}}{\partial\kappa_3} & \text{for } i=3 .\end{cases} \tag{A5}$$

Because $\partial\omega/\partial k_i$ is identical to the ith component of the group velocity we have established the statement given at the beginning of this appendix.

[1]B. Taylor, H. J. Maris, and C. Elbaum, Phys. Rev. Lett. 23, 416 (1969).
[2]B. Taylor, H. J. Maris, and C. Elbaum, Phys. Rev. B 3, 1462 (1971).
[3]See, for example, H. Kinder, J. Weber, and W. Dietsche, in *Proceedings of the Third International Conference on Phonon Scattering in Condensed Matter,* edited by H. J. Maris (Plenum, New York, 1980), p. 173; A.F.G. Wyatt, *ibid.,* p. 181.
[4]See, for example, G. A. Northrop and J. P. Wolfe, in *Proceedings of the Third International Conference on Phonon Scattering in Condensed Matter,* edited by H. J. Maris (Plenum, New York, 1980), p. 377; J. C. Hensel and R. C. Dynes, *ibid.,* p. 395.
[5]J. C. Hensel and R. C. Dynes, Phys. Rev. Lett. 43, 1033 (1979).
[6]G. A. Northrop and J. P. Wolfe, Phys. Rev. Lett. 43, 1424 (1979).
[7]G. A. Northrop and J. P. Wolfe, Phys. Rev. B 22, 6196 (1980).
[8]H. J. Maris, J. Acoust. Soc. Am. 50, 812 (1971).
[9]L. D. Landau and E. M. Lifshitz, *Fluid Mechanics* (Pergamon, New York, 1959) Chap. 8.
[10]P. Taborek and D. Goodstein, Solid State Commun. 33, 1191 (1980).
[11]P. Taborek and D. Goodstein, Phys. Rev. B 22, 1550 (1980).
[12]V. T. Buchwald, Proc. R. Soc. London Ser. A 253, 563 (1959).
[13]A. G. Every, Phys. Rev. Lett. 42, 1065 (1979).
[14]The values of elastic constants and density of Ge employed in the calculation are $c_{11}=1.318\times10^{12}$ dyn/cm^2, $c_{12}=0.496\times10^{12}$ dyn/cm^2, $c_{44}=0.685\times10^{12}$ dyn/cm^{12}, and $\rho=5.34$ g/cm^3. See H. J. McSkimin, J. Appl. Phys. 24, 988 (1953).
[15]For dependence of phonon flux on detector shape and size, see M. Lax and V. Narayanamurti, Phys. Rev. B 22, 4876 (1980).
[16]F. Rösch and O. Weis, Z. Phys. B 27, 33 (1977).
[17]W. E. Bron and W. Grill, Phys. Rev. B 16, 5303 (1977).
[18]The phase velocities 5.24×10^5 cm/sec (longitudinal phonons), 3.10×10^5 cm/sec (transverse phonons), and mass density 8.80 g/cm^3 are employed for Constantan (isotropic). See Ref. 16.